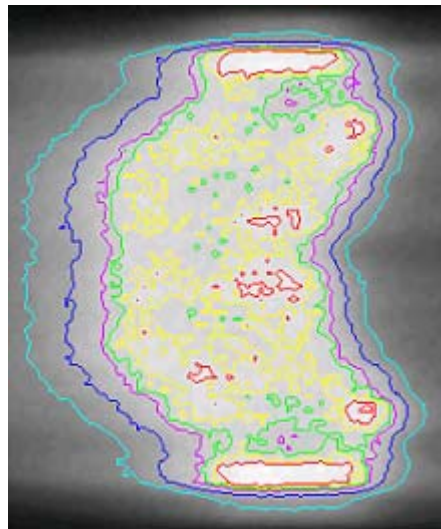


A POLYMER GEL PREPARED UNDER NORMAL LEVELS OF OXYGEN

- BASIC STUDIES AND THE POTENTIAL FOR IMRT VERIFICATIONS

Master of Science Thesis



**Anna Karlsson
Department of Radiation Physics
Lund University
Malmö University Hospital**

Supervisor: Ph. D. Sven Å.J. Bäck

Abstract

Introduction

The technology for planning and delivering radiotherapy has in the last decade undergone some revolutionary development and it is now possible to perform complex treatments such as stereotactic treatments and treatments using dynamic wedges, multileaf collimator and intensity modulation. The more precise limits surrounding the PTV have made it of utmost interest to be able to verify calculated dose distributions in 3D. For this purpose gel dosimetry along with MRI has shown to be suitable. In this thesis a new type of gel was used and its basic characteristics evaluated. This polymerisation-based gel can be produced and stored under normal levels of oxygen. The potential for the gel dosimetry system was pointed out for 3D verification of IMRT.

Materials and methods

The components of the gel are water, gelatine, methacrylic acid, ascorbic acid and copper sulphate. The mixing procedure was performed in a fume cupboard and the time needed for the manufacturing was approximately 2 h. As a result of the radiation induced polymerisation the NMR relaxation rates for the water protons in the gel are increased with absorbed dose. Screw-top glass vials were used when evaluating dose response characteristics e.g. dynamic range, magnetic field dependence, and the use of different types of methacrylic acids. The vials were also used for absorbed dose calibration. For the IMRT verification a cylindrical shaped glass bottle was used. The dose distribution measured with the polymer gel was compared with the distribution calculated by the treatment planning system Helios, CadPlan. Isodoses were used for evaluation.

Results and discussion

For this new type of polymer gel the dynamic range was found to be greatly extended compared to former polymer gels. As for other polymer gels it was shown that the purity grade of the components was crucial for the dose response. Further, the slope and the intercept were found to be decreased for increased magnetic field strength. It was shown that the gel has great potential for verification of treatments like IMRT. In the comparison between the measured and the by the treatment planning system calculated relative absorbed dose map it was found that the absorbed dose isodoses agreed mostly within 2 mm. However, there is a need of improved image/matrix evaluation methods for the 3D verification of the treatment planning system calculated dose map, both spatial and regarding dose levels.

Abbreviations

TPS	Treatment planning system
MLC	Multileaf collimator
IMRT	Intensity modulated radiation therapy
PTV	Planning target volume
TLD	Thermoluminescent dosimeter
3D	Three dimensions
MRI	Magnetic resonance imaging
OPoG	Oxygen polymer gel
PoG	Hypoxic polymer gel
NMR	Nuclear magnetic resonance
T1	Spin-lattice relaxation time, longitudinal relaxation time
T2	Spin-spin relaxation time, transversal relaxation time
1/T1=R1	Spin-lattice relaxation rate, longitudinal relaxation rate
1/T2=R2	Spin-spin relaxation rate, transversal relaxation rate
CT	Computer assisted X-ray tomography
Fe³⁺	Ferric ions
Fe²⁺	Ferrous ions
FeMRI	Fricke solution mixed with gelling substance evaluated using MRI
BIS	N,N'-methylene-bisacrylamid
MAA	Methacrylic acid
AA	Ascorbic acid
Cu²⁺	Copper (II) ions
TE	Echo time
RF	Radio frequent
OAR	Organs at risk
TR	Repetition time
FoV	Field of View
IDL	Interactive data language software (Version 5.4, Research Systems Inc., Boulder, CO, US)

Contents

1	INTRODUCTION.....	5
2	AIM	6
3	BACKGROUND	6
4	THEORY	8
4.1	POLYMER GEL.....	8
4.1.1	<i>Principles of polymer gel dosimetry.....</i>	8
4.1.2	<i>Chemical reactions.....</i>	8
4.2	NMR/MRI	9
4.2.1	<i>NMR dose response and T2 calculation.....</i>	9
4.2.2	<i>MRI non-uniformity.....</i>	10
4.3	IMRT AND THE TREATMENT PLANNING SYSTEM	10
5	MATERIALS AND METHODS	12
5.1	GEL MANUFACTURING	12
5.1.1	<i>Dosimetry gel</i>	12
5.1.2	<i>MRI non-uniformity study</i>	13
5.2	TREATMENT PLANNING.....	14
5.3	IRRADIATION	14
5.4	MAGNETIC RESONANCE IMAGING	15
5.5	EVALUATION	15
5.5.1	<i>Image matching.....</i>	15
5.5.2	<i>Image and data processing</i>	15
	RESULTS AND DISCUSSION.....	16
5.6	GEL MANUFACTURING	16
5.7	DOSE RESPONSE.....	16
5.8	MRI NON-UNIFORMITY	22
5.9	IMRT VERIFICATION	22
	CONCLUSIONS.....	25
6	ACKNOWLEDGEMENTS	26
7	REFERENCES.....	27

1 Introduction

Radiation therapy is an established treatment for different types of tumour diseases. It is used both for curative and palliative purposes, often together with surgery and/or pharmaceuticals. Radiation therapy is rather inexpensive compared with medicine and other types of treatments [1].

During the last decade the linear accelerators and the treatment planning systems (TPS) have undergone immense development and it is now possible to perform complex conformal treatments such as stereotactic treatments and treatments using dynamic wedges, multileaf collimators (MLC) and intensity modulation (IMRT).

The knowledge of the true dose distribution is of great importance. The purpose is a well-defined and homogeneous absorbed dose to the tumour with appropriate margins, and as low dose as possible to the healthy tissue to prevent side effects [2]. The dose gradients around the planning target volume (PTV, [3]) tend to be steeper and more precise with the new types of treatment regimes. This makes it of utmost interest to verify the treatments. In general dosimeters such as ionization chambers, diodes, thermo luminescent dosimeters (TLD) and radiographic film along with suitable phantoms are used for dose verification. These measuring instruments measure the dose in one point at the time or, as in the case for the film, in one plane at the time. To obtain the dose distribution in three dimensions (3D) several measurements, or dosimeters, are needed. The procedures are laborious and time-consuming, and may not lead to a dose map with sufficient high spatial resolution (except for the film). Possible steep dose gradients will thus be difficult to detect. The conventionally used detectors are non-tissue equivalent, which leads to perturbation of the radiation field. Some of these detectors do also suffer from radiation quality dependence, as well as dependence of the irradiation direction. To be able to produce 3D maps of the dose with high spatial resolution there is a need for another type of dosimeter systems. For this purpose the gel dosimeter in combination with Magnetic Resonance Imaging (MRI) has shown to be suitable [4].

The gel together with MRI as dosimeter system has many advantages. It is independent of radiation direction; quality and dose rate for conventional clinical beams and it is truly 3D measuring [5]. The phantoms are filled with gel and they can be made in almost any shape, to mimic any human body part. Since the gel is soft tissue equivalent [6][7], there is no need for perturbation corrections. The spatial resolution is that of the procedure of MRI (<1 mm). The system is also capable of integrating absorbed dose contributions both in time and space, which is of great importance for the IMRT dose verification.

2 Aim

The aims of this study were to:

- Develop the preparation of a new type of polymer gel (OPoG) that can be manufactured under normal levels of oxygen.
- Examine the NMR dose response for various methacrylic acids and different magnetic field strengths.
- Evaluate the MRI signal non-uniformities for various simulated dose levels.
- Investigate absorbed dose calibration for R2, spin-spin relaxation rate ($1/T_2$), and R1, spin-lattice relaxation rate ($1/T_1$). The calibration involves estimation of uncertainties.
- Verify a complete radiotherapy procedure for an IMRT set up using the elementary phantom chosen. This procedure involves CT-scanning, treatment planning and irradiation.

3 Background

1984 the first paper related to gel dosimetry using MRI was published [8]. The first type of gel dosimetry was Fricke solution mixed with gelling substance. Thereby spatial dose information could potentially be obtained by MRI. In the paper by Gore *et al.*, they found that the nuclear magnetic resonance (NMR) parameter R1 ($1/T_1$) was linearly correlated with the amount of ferric ions (Fe^{3+}) produced by irradiation of a ferrous (Fe^{2+}) solution. The dosimetry system of using Fricke solution mixed with gelling substance and evaluated with MRI (FeMRI) has proved to be a reliable measuring instrument for the dose distribution in 3D [4]. It is rather easy to prepare. The grand disadvantage of FeMRI is the diffusion of the iron ions that destroys the dose distribution information by time [9]. This can be a problem for certain applications, for example when steep dose-gradients are evaluated.

A new kind of dosimetry gel system, PoG [10], was introduced in 1993. These gels consisted of water, gelatine, a monomer (acrylamide) and a “cross-linker” (BIS-acrylamide monomers). Irradiation caused the monomers to polymerise and the spin-spin relaxation time was reduced [11]. These polymerisation-based systems do not suffer from the diffusion problem. PoG has to be prepared, stored and used under hypoxic conditions, which means that oxygen must not come in contact with the gel. Oxygen has an inhibiting effect on the radicals in the gel [12]. The chemicals used are also very toxic. These eccentricities make the preparation laborious and cumbersome.

Fong *et al.* have introduced a new type of polymer gel, here referred to as OPoG. This new gel does not suffer from the oxygen problem that is associated with PoG. The chemicals used are also less toxic [7]. The manufacturing of this gel is easier, and the materials chosen for phantoms are potentially not that critical. The active substances of this gel based on gelatine were methacrylic acid, hydroquinone, copper sulphate and ascorbic acid.

The spin-spin relaxation rate R2 ($1/T_2$) and the spin-lattice relaxation rate R1 ($1/T_1$) are linearly related to the absorbed dose for both OPoG [13] and PoG [14]. However, the sensitivity is much higher for R2, and that is why this is the parameter generally used for evaluation. Linearity has been reported for absorbed doses between 0 and 40 Gy [13]. Thus the linearity range is extended for OPoG compared to PoG. For PoG the linearity range has been reported to be between 0 and 8 Gy [11][14].

The slope and the intercept of the dose response depend of the concentrations of the different compounds as well as the magnetic field strength [7]. Problems like inhibition of polymerisation and auto-polymerisation have appeared when using various chemicals; this is probably because of impurities in the chemicals used [13]. The fact that the purity grade of the chemicals used affects the dose response has previously been reported for PoG [14].

At present MRI is the most frequently used method for evaluation of dosimetry gels in 3D. A more accessible and cost effective system could maybe take the polymer gel dosimetry system in to the clinic. Alternative evaluation methods are FT-Raman spectroscopy [15], optical CT-scanning [16], x-ray CT [17] and ultrasound [18].

4 Theory

4.1 Polymer gel

4.1.1 Principles of polymer gel dosimetry

There are some fundamental principles for gel dosimetry using MRI evaluation. The chemical reactions initiated by radiation leads to the formation of polymers. As a result of the polymerisation the relaxation rates for the water protons in the gel are increased. Thus, there is a difference in NMR properties in the gel before and after the irradiation [19]. The magnitude of this difference is related to the absorbed dose. The NMR parameter measured T_2 as a function of absorbed dose follows a double exponential relationship. However the commonly used parameter for absorbed dose calibration is R_2 ($1/T_2$) (fig. 1), due to the pseudo-linear correlation with absorbed dose [12]. This pseudo-linearity is hereafter referred to as linearity.

The gelatine serves as a three dimensional network, which retains the gel solution. This is needed to sustain the spatial information of the absorbed dose in three dimensions.

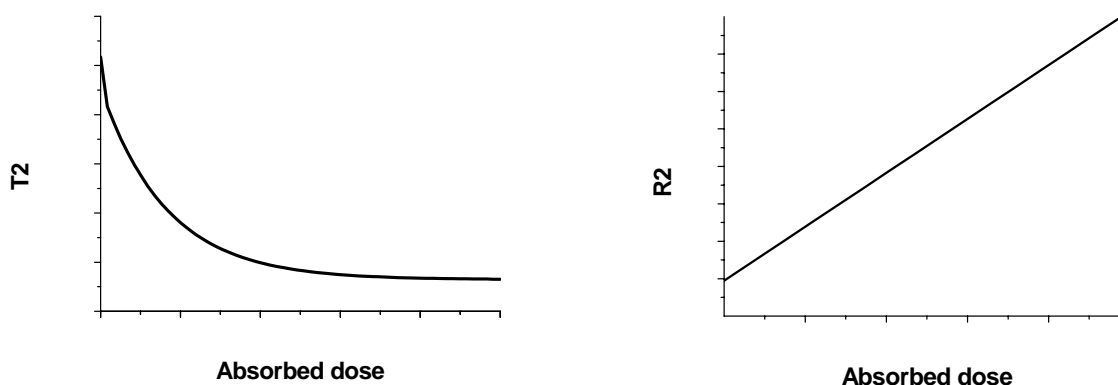


Figure 1. Schematic plots of T_2 (left) and R_2 ($1/T_2$) (right) as a function of absorbed dose.

4.1.2 Chemical reactions

OPoG is an aqueous solution of gelatine mixed with methacrylic acid (MAA), copper sulphate and ascorbic acid (AA). There are only two introductory studies on this type of gel [7][13]. A kinetic study of the polymerisation of methyl acrylate in aqueous medium containing oxygen, ascorbic acid and copper(II) has been reported [20]. The principles of the polymerisation are expected to be of a similar kind in the dosimetry gel, though there is gelatine present.

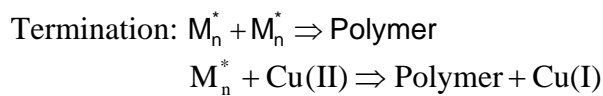
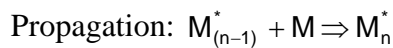
Polymer gels based on methacrylic acid are known to lead to a higher slope for the R_2 dose response compared with other monomers [28][7].

Reaction mechanisms

It is believed that the complex of Cu(II), ascorbic acid and oxygen with radiolysis of water serves as a free radical source for the initiation of the polymerisation of methacrylic acid [7].



These free radicals, R, can react with monomers, M, and form monomer radicals, M*, (initiation). It is also likely that formation of gelatine radicals take place. This step is followed by propagation or termination. Propagation involves creation of polymer radicals, termination occurs when two polymer radicals neutralize each other or a polymer radical reacts with Cu(II), and the chain propagation stops [7][20].



It is also believed that molecules of the gelatine can terminate polymerisation. It can be concluded that the irradiation-initiated polymerisation of the OPoG is not fully understood.

The G-value is defined as the amount of molecules that are changed or products that are formed, for every 100 eV of absorbed energy in the system [12]. For the polymer gels the G-value is approximately 10^5 [12]. This high G-value is due to the chain reaction of the polymerisation that occurs in the gel by irradiation. (Fricke gels have a G-value of approximately 45 [21])

4.2 NMR/MRI

4.2.1 NMR dose response and T2 calculation

The parameter measured with MRI for OPoG is most commonly T2. The relation between T2 and absorbed dose is a double exponential function. For the dose interval used in general a linear relation between R2 and absorbed dose can be utilized.

When measuring T2 images a series of spin echo images was used. These images were obtained by a multi spin echo sequence. T2 determines the rate of the signal decrease when the echo time (TE) is varied. The signal amplitude (S) and the echo time (TE) are related in the following way according to the signal equation:

$$S = k \cdot e^{-\frac{\text{TE}}{\text{T2}}}$$

Where k is a constant depending on the object and the configuration of the MRI-system. By varying TE, T2 can be calculated from the equation. The calculations were performed by using the PMRelax PC software developed at the department [22]. Noise was considered by not using signal images with not sufficient visibility of the area of interest for T2 calculations.

For the Praxis analyser a spin echo (Hahn echo) sequence was used for T2 measurements. The T1 measurements were performed using a saturation recovery sequence. The Praxis analyser

provides no spatial information. Both T2 and T1 were calculated by the Praxis analyser software.

4.2.2 MRI non-uniformity

If not corrected for, non-uniformities of R2 in the images lead to areas of over- and under-estimations of the dose. The main reason for non-uniformities is an inhomogeneous RF-field. It has been reported for a homogenous phantom [23] that the R2 map was uniform within an area of 120 cm² in the centre of the coil. This was true when using a multi-echo sequence in combination with a circularly polarized head coil for T2 imaging. Near the edges of the coil the R2 values decrease considerably. This non-uniformity was not seen when using the body coil. However using the body coil is at the cost of signal-to-noise.

Non-uniformities can also arise from temperature inhomogeneities in the phantom during scanning [24]. These temperature inhomogeneities can be reduced by storing the phantom in the scanning room for temperature equilibration before scanning. However, the temperature increase caused by the RF energy of the excitation and refocusing pulses can still be a problem [23].

A practical way to correct for non-uniformities in the R2 map is to scan a homogenous phantom e.g. the gel phantom before irradiation, and then use these images as a template to correct the present R2 images [25][14].

4.3 IMRT and the treatment planning system

Intensity modulated therapy is the most advanced type of conformal radiotherapy [5]. The conventional radiotherapy using rectangular shaped fields along with blocks and wedges were improved by the development of the MLC. By using MLC even more advanced geometrically shaped fields can be shaped, i.e. conformal radiotherapy. It also makes it easier, less time consuming and more ergonomic, to shape the fields. Two commonly used ways of generating intensity-modulated fields involve MLC, multiple-static MLC (“step and shoot”) and dynamic MLC (DMLC, “sliding window”) [5]. In the step and shoot technique, the beam is turned off during leaf movement, whilst in the case of sliding window the individual leaves are moved continuously during irradiation.

The strength with IMRT is the concave dose distributions that rather easy can be produced, such distributions benefit several types of treatments e.g. for head-and-neck, prostate and breast tumours [5]. When sparing more volume of organs-at-risk (OAR, [3]), the absorbed dose to the PTV can be increased and thereby the treatment result can be improved.

Helios™ is the inverse planning tool used in this thesis for IMRT and it employs the same beam data and dose calculation algorithms as used in standard CadPlan™ software (Varian Medical systems, Palo Alto, CT). When using inverse planning for DMLC IMRT the treatment planning system (TPS) calculates the trajectories of the leaves (Helios) and the dose distribution (CadPlan). The user predefines the number of fields and their collimator and gantry angles.

For the treatment plan that was made for the IMRT verification in this thesis the calculation model used was a single pencil beam model for photons [26].

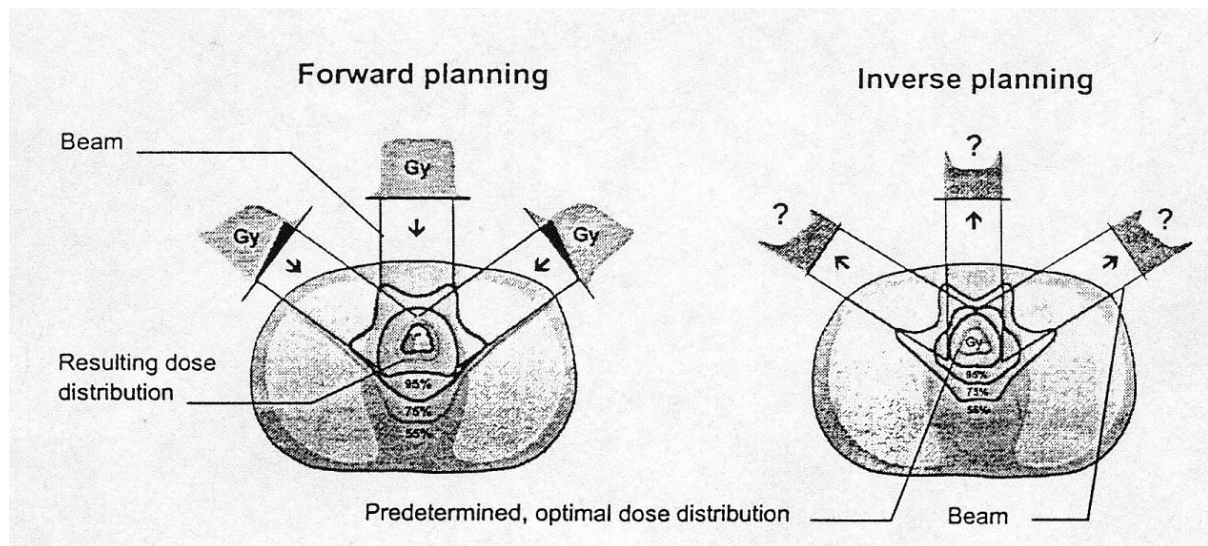


Figure 2. Schematic illustration of the difference between forward planning and inverse planning. (The figure is from [26])

Uncertainty needed according to ICRU

In areas relevant for the treatment the computer calculated dose should not differ from the measured dose by more than 2 %. For steep dose gradients the difference in position of isodose lines should be less than 2 mm [27].

5 Materials and methods

5.1 Gel manufacturing

5.1.1 Dosimetry gel

The constituent elements of the gel were methacrylic acid (different types from Sigma were used), gelatine (Swine skin, 300 Bloom, Sigma Aldrich), ascorbic acid (minimum 99%, Sigma Aldrich), copper sulphate (pentahydrate, 98+%, Sigma Aldrich) and ultra pure deionised water (table 1).

Table 1. *The gel composition (w/w).*

Chemical	Concentration
Water	83.9% w/w
Gelatine	8% w/w
Ascorbic Acid	2×10^{-3} M
Copper sulphate	3.3×10^{-4} M
Methacrylic acid	8% w/w

This type of gel has previously been suggested [7]. However, the concentrations of the different compounds were slightly modified and hydroquinone¹ was excluded in compliance with prior investigations at the department. Still, the methacrylic acid used, contains a minor amount of hydroquinone (100-250 ppm) to prevent auto-polymerisation on the shelf. The purpose of using hydroquinone is to reduce free radicals that can have been introduced from the gelatine and/or other constituents of the gel [7] and by that lower the intercept for the calibration curve.

Preparation

The mixing procedure was performed in a fume cupboard, in air under normal levels of oxygen. The gelatine was added to the room temperature water. Before heating the gelatine was allowed to swell from soaking for ~10 min. The mixture was heated under stirring. To make sure that the gelatine is totally dissolved the temperature 45° C was held for approximately an hour, until the mixture was clear and homogeneous. The heat was then turned off and the solution was allowed to cool down. At the temperature ~35° C the ascorbic acid (solved in water), the CuSO₄ (solved in water) and the methacrylic acid were added. Finally, the prepared gel was poured into the phantoms. The gel was left in room temperature over night in order to set. For



Figure 3. *A picture of the equipment used when mixing the gel.*

the IMRT measurements an ordinary cylindrical formed glass bottle was used (1500 ml, diameter~11 cm). The size of the IMRT phantom was a compromise between two matters. The phantom must fit into the head coil of the MRI scanner in order to obtain higher

¹ Hydroquinone is a free radical scavenger.

signal-to-noise ratio then in the case of using the body coil. However, the phantom needed to be large enough to contain a suitable target. Screw-top glass vials (12 ml, diameter~2 cm) were used for dose response evaluation (fig. 7).

5.1.2 MRI non-uniformity study

For the non-uniformity study two homogenous phantoms were prepared simulating 0 respectively 30 Gy. The simulation was based on T2 values, and was performed by using ordinary compounds of the gel. In different amounts though, to give the same T2 values as if the gel had been irradiated homogeneously to the two different absorbed doses. T1 effects were disregarded. A study of T2 dependence for gelatine and Cu(II) was performed. The result of the investigation is shown in the figure 4. The purpose of these studies were not to achieve the exact amounts of gelatine and Cu(II) for a specific T2, but to give an estimation of the right amounts to use to approximately attain the chosen doses.

Preparation

The gelatine was poured into the deionised water. After the gelatine has swelled from soaking the mix was heated under stirring to ~ 45° C. Then the mix was allowed to cool down to ~35° C before the copper sulphate (solved in water) was added. The gel was then poured into the phantom (the same as for the IMRT verification study). The phantom was left at room temperature to allow the gel to set.

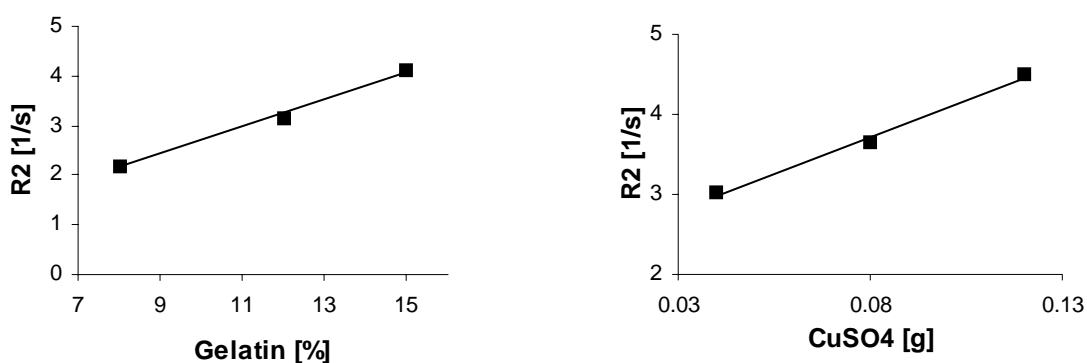


Figure 4. T2 for different gelatine and Cu(II) concentrations in the gel. The evaluation was performed using the Praxis analyser.

Table 2. Composition of the gels (1500 g) for the non-uniformity study.

Chemicals	"0 Gy"	"30 Gy"
Water	1319,9 g	1319,0 g
Gelatine	180 g, 12%	180 g, 12%
Copper sulphate	1.78x10 ⁻⁴ M (0.0665 g)	2.67x10 ⁻³ M (1.0 g)

5.2 Treatment planning

The treatment planning was performed at Copenhagen University Hospital using the Helios™/CadPlan™ software (Varian medical systems, Palo Alto, CT).

The phantom was CT scanned to obtain input data to the treatment planning system. The entire volume was scanned in 3 mm thick slices. During the scanning the phantom was water filled. Since the gel contains nearly 84 %, this was assumed not to have any significant effect on the treatment plan.

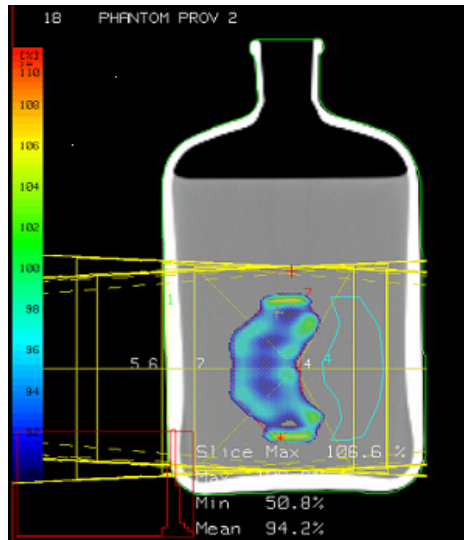


Figure 5. The isocentric slice of the water filled phantom from the treatment planning system.

The treatment plan was based on seven co-planar fields. The target was planned to receive 16.5 Gy at the normalisation point, with a minimum dose 14 Gy and maximum dose 18.6 Gy. The target was contoured with the shape of a kidney, or a “C” (fig. 5). As discussed earlier concave dose distribution is one of the benefits with IMRT. Thus, it was suitable challenge to choose this shape of the target. Adjacent to the target an OAR was placed (fig. 5). The maximum dose allowed for the OAR was set to 7.1 Gy and the minimum to 0 Gy.

5.3 Irradiation

The irradiation of the IMRT phantom was carried out at Copenhagen University Hospital, using a Varian Clinac 2300 C/D (120 leafs DMLC). The technique used for IMRT was sliding window. The energy for the photon beams was 6 MV. The vials used for dose response evaluation were irradiated at the same occasion as the IMRT phantom, also using 6 MV photons. The vials were irradiated in a large water phantom. The water phantom was made especially for the purpose of dose response irradiations. The holes for the vials were positioned with their centres at the depth of 2.7 cm. The percentage depth dose were 96 % at this depth.

All other absorbed dose response irradiations for the different batches were performed at Malmö University Hospital. The 12 ml screw-top glass vials containing gel were irradiated in the same water phantom mentioned above using 18 MV photons (Varian Clinac 2100c). The holes for the test tubes were placed with their centres at the depth for the dose maximum for the 18 MV photons, 2.7 cm.



Figure 6. The irradiation arrangement.

5.4 Magnetic Resonance Imaging

The MRI was performed approximately 24 h after the irradiation. It is known for former gels (PoG) that the post-irradiation polymerisation lasts for at least 12 hours after the irradiation [33]. The same was assumed to be true for OPoG. To prevent any temperature gradients in the phantom the phantom was placed in the scanning room ~10 hours before the measurement. The scanning was performed on a 1.5 T scanner (Magnetom, Vision, Siemens, Erlangen, Germany) with a Multi Spin Echo sequence. The repetition time (TR) was 3000 ms and the echo time was between 22.5 ms and 720.0 ms and the inter-echo time was 22.5 ms. The acquisition time was approximately 30 minutes with two excitations, FoV=256 mm x 256 mm and a pixel size of 1.0 x 1.0 mm². The slice thickness was 3 mm and the transversal slices were acquired at the same positions as the CT-slices. The number of slices obtained was 12. The sequence was run three times, with four slices acquired from each measurement. In order to avoid cross-talking between the slices they were separated by 3 mm, adjacent slices were not scanned in the same sequence. The vials for the dose response calibration for the IMRT measurement were scanned as well. They were placed in a plastic-stand when scanned.

The non-uniformity study was evaluated using the same MRI acquisition protocol as for the irradiated phantoms. Three slices were obtained, one through the centre of the phantom and two with 10 mm offset (+/-).

A pulsed NMR analyser with a permanent magnet of 0.25 T was used for the analysis of the dose response (Praxis II, Praxis corp., USA). T2 was measured using a 90°-180° sequence (Hahn echo) and for T1 a 90°-90° sequence (saturation recovery) was used. The relaxation curve was obtained by varying the time between the radio frequency pulses. The time between the acquisitions was referred to as step time, the number of acquisitions was 32 and the number of excitations for the measurements was two. The T2 measurements were performed with a repetition time (TR) of 6 s and a step time of 0.3 ms. When measuring T1 the corresponding values were 6 s and 15 ms, respectively.

All measurements were carried out at room temperature.

5.5 Evaluation

5.5.1 Image matching

The pixel size of the images from the treatment planning system was scaled from 1.25 x 1.25 mm² to 1.0 x 1.0 mm². Thus the pixel size was the same as for the MRI measurements. The images, from the TPS and MRI, were matched with the edges of the phantom as reference. The scaling and the matching were performed using the in-house developed software PMRelax.

5.5.2 Image and data processing

The isodoses were based on the median filtered (kernel 3x3) relative absorbed dose map. When using median filter isolated high and/or low values are removed. But it does not blur edges larger than the chosen neighbourhood, which is important for these types of images where steep (dose) gradients are present. The isodoses and the filtering were performed using the IDL (Interactive Data Language, Version 5.4, Research Systems Inc., Boulder, CO, US) software.

Results and discussion

5.6 Gel manufacturing

The manufacturing method of gels has been greatly simplified by using OPoG compared with PoG. The mixing procedure is far less time consuming, mostly because there is no need to prevent the gel from exposure to oxygen. Another benefit is the less toxic components [7].

The total time for the mixing procedure is approximately 2 hours. For large volumes the time needed to allow the gel to set was several hours, whereas the gel was set after approximately 30 min for the small screw-top vials.

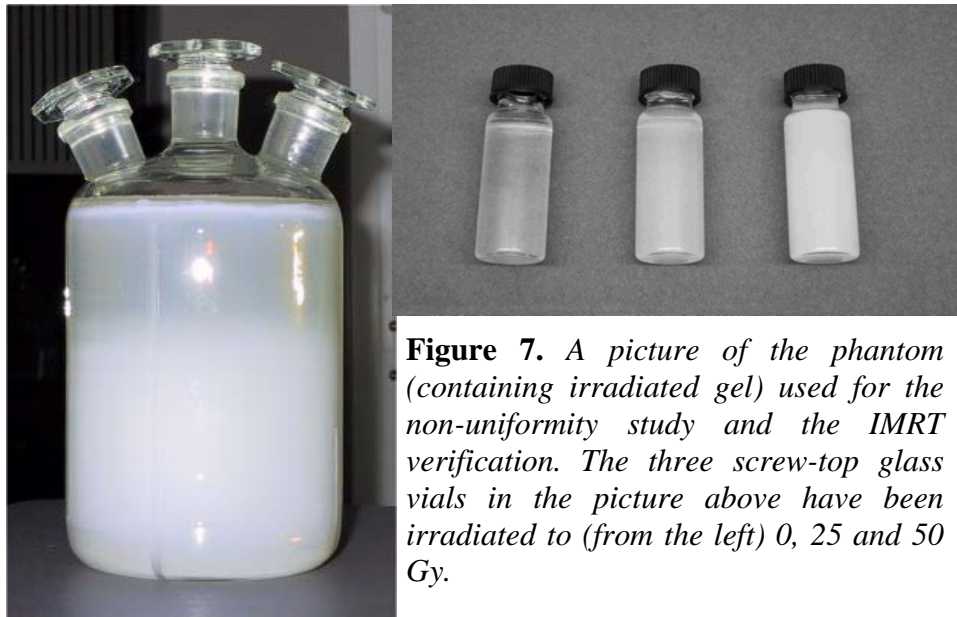


Figure 7. A picture of the phantom (containing irradiated gel) used for the non-uniformity study and the IMRT verification. The three screw-top glass vials in the picture above have been irradiated to (from the left) 0, 25 and 50 Gy.

5.7 Dose response

The R2 and R1 absorbed dose response for the OPoG were compared (fig. 8). The difference of the slope for the two NMR parameters was found to be of approximately the same magnitude (factor ~ 10) as for PoG [14]. The higher slope and intercept measured, both for R2 and R1 compared to the study carried out by Gustavsson *et al* are probably due to the different amounts of methacrylic acid used (table 3). The fact that the slope and the intercept are increased by higher amount of methacrylic acid has been verified by others [7].

There was an approximately linear dose response for R2 to about 40 Gy (fig. 8 and 9). This correlates well with previous results for OPoG [13]. Thus, the linearly dose response was found to be considerably extended compared with PoG. Linearity up to about 8 Gy has previously been reported for PoG [11], [14]. This indicates that the dose resolution can potentially be further optimised for these new types of gels [13], i.e. the uncertainty can be improved. For higher absorbed doses the slope was found to decrease (fig. 9) and the linear approximation of R2 vs. absorbed dose was not valid. However the dynamic range was found to extend to at least 100 Gy (fig. 9). A polynomial fit may be used for the dose response of R2 or a double exponential fit can be used for T2 (c.f. [29]). The useful range for the relative measurements without introducing a calibration process requires a linear response thus the useful range was found to be 0- 40 Gy.

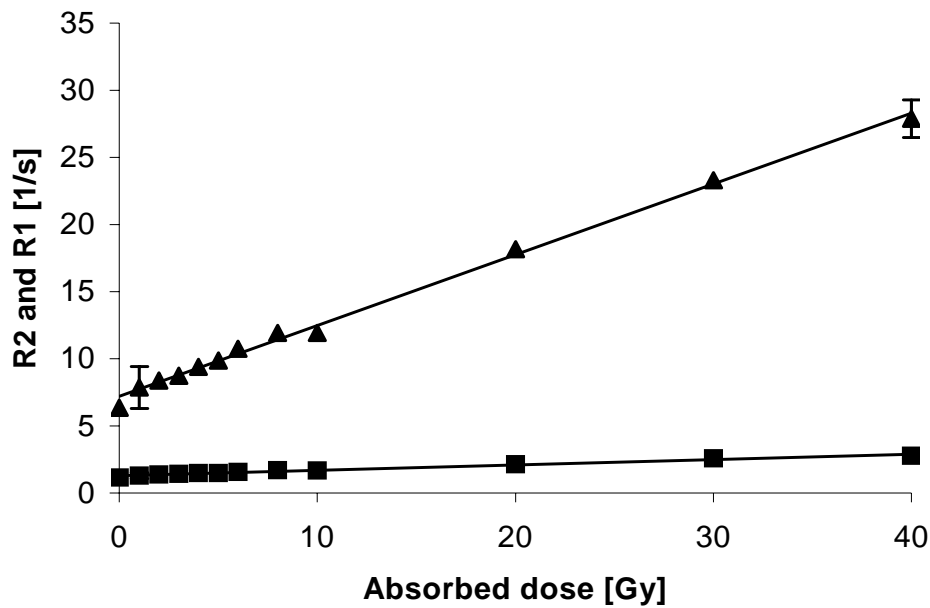


Figure 8. R_2 (▲) and R_1 (■) as a function of absorbed dose for one preparation. The evaluation was performed using the Praxis analyser. Slopes and intercepts in table 3. (MAA (M 0782) 8 %, AA 4×10^{-3} M, CuSO_4 6.6×10^{-4} M).

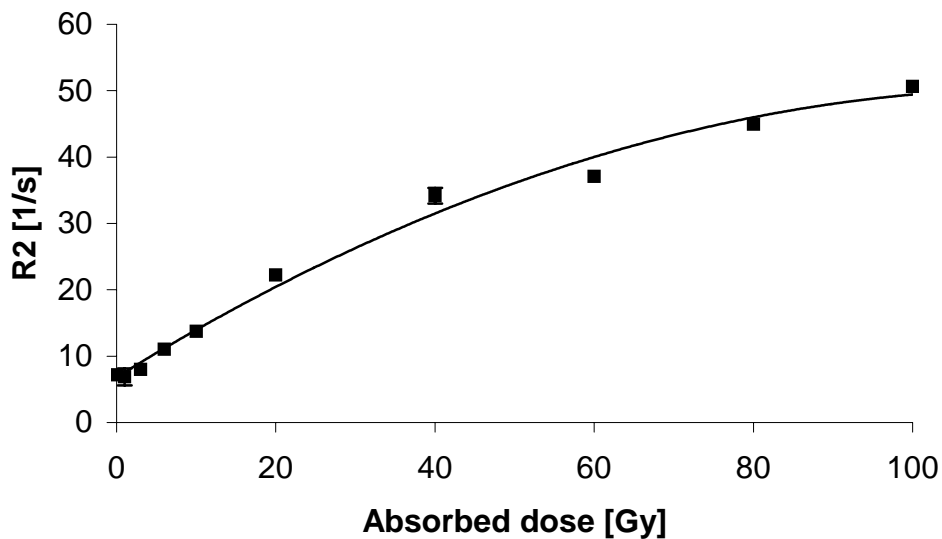


Figure 9. R_2 (■) as a function of absorbed dose. The evaluation was performed using the Praxis analyser. (Methacrylic acid 39.53748 %, AA 4×10^{-3} M, CuSO_4 6.6×10^{-4} M). The expression for the polynomial fit: $y = -0.0032x^2 + 0.74x + 6.8$ ($R^2 = 0.99$).

The slope and the intercept decreased with increased magnetic field strength (fig. 10). This corresponds well to former reports for both PoG [14] and OPoG [13]. One reason for this may be that the NMR correlation time is decreased by an increased magnetic field strength, and therefore T_2 is increased and consequently R_2 is decreased [14]. However others suggest the reverse relationship [12][10]. This incompatibility may be due to different temperatures during evaluation and/or that the gels are of different compositions [14]. In OPoG the paramagnet species Cu(II) also have magnetic field strength dependence. Further studies are

needed for the understanding of the magnetic field strength dependence for the dose response of OPoG. Inter-calibration of the R2 measuring devices has to be performed before final conclusions can be drawn.

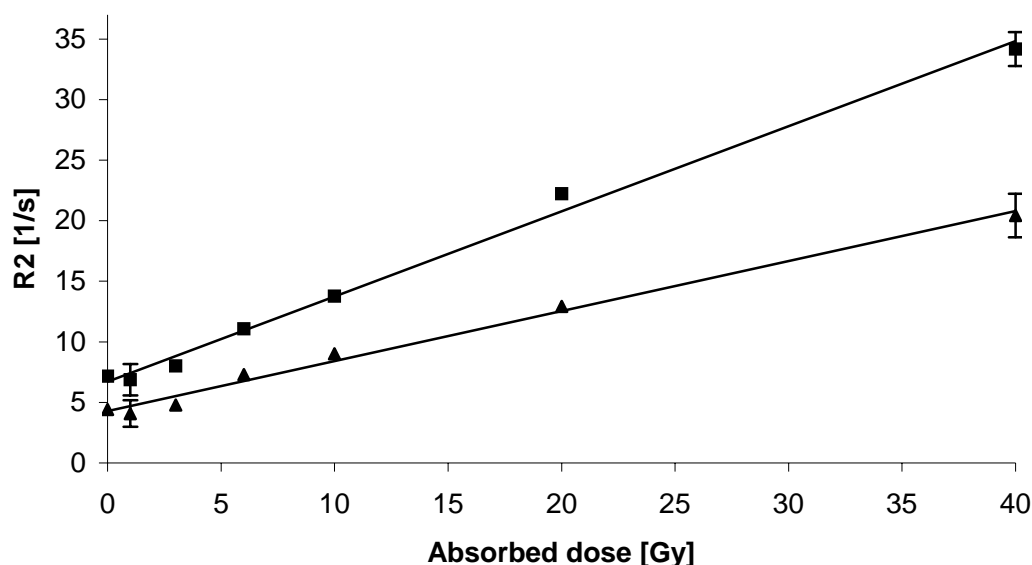


Figure 10. R2 as a function of absorbed dose as obtained using the Praxis analyser, 0,25 T (■), and the MRI-scanner, 1,5 T (▲). The measurements were performed the same day. (MAA (39 537 4) 8 %, AA 4×10^{-3} M, CuSO_4 6.6×10^{-4} M). The error bars shown are discussed further below.

Table 3. Slopes and intercepts for the graphs in figure 8 and 10 and reported results. R is the correlation coefficient (0-40 Gy).

R2 or R1	[T]	MAA [%]	Slope [$\text{s}^{-1}\text{Gy}^{-1}$]	Intercept [s^{-1}]	R ²	REF
R1	0.25	8	0.04	1.3	0.980	fig. 8
R1	0.25	6	0.038	0.74	0.996	[13]
R2	0.25	8	0.53	7.2	0.996	fig. 8
R2	0.25	8	0.70	6.72	0.994	fig.10
R2	0.25	6	0.41	3.20	0.996	[13]
R2	0.5	9	0.51	4.63	-	[7]
R2	1.5	8	0.41	4.3	0.991	fig. 10
R2	1.5	6	0.30	2.12	0.999	[13]

Several types of methacrylic acids and their influence on the absorbed dose response were examined (fig. 11, table 4). Distinction was found between two groups. The slopes for the two groups are approximately the same, but the intercepts were somewhat different. This may be a result depending on different concentrations of hydroquinone in the methacrylic acids. However one would expect the reversed relationship (c.f. Fong *et al*) i.e a lower intercept (background). It is only the number IV methacrylic acid that gives rise to a dose response that is linear from 0 Gy absorbed dose (fig. 8, 11 and 12). Dependence of the purity grade for the

different ingredients in the gel regarding the absorbed dose response has also been reported for PoG [14].

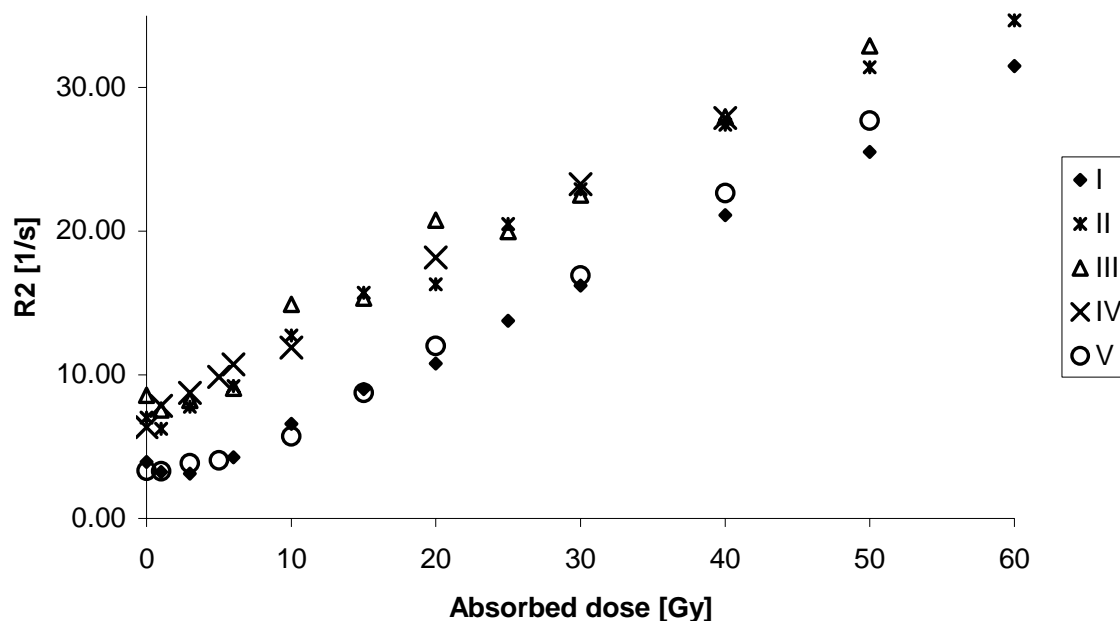


Figure 11. Dose response for different types of methacrylic acids (table 4). The evaluation was performed using the Praxis analyser.

Table 4. The different methacrylic acids used. All of them are from Sigma. Methacrylic acid I and V are from different batches.

Methacrylic acid (product number)	Monomer purity	Hydroquinone [ppm]	Slope [s ⁻¹ Gy ⁻¹]	Intercept [s ⁻¹]	R ²
I (39 537 4)	99 %	100-250	0.474	2.158	0.994
II (15 572 1)	99 %	250	0.488	7.089	0.989
III (640 50)	≥98 %	250	0.483	8.137	0.978
IV (M 0782)	99 %	250	0.530	7.093	0.997
V (39 537 4)	99 %	100-250	0.505	2.050	0.992

The main difference between PoG and OPoG is the presence of ascorbic acid and Cu(II) in OPoG. An investigation of the dose response dependence for different concentrations of these components was thus performed (fig. 12). For higher concentrations of ascorbic acid and copper sulphate the intercept was increased and the slope was decreased. The increased intercept was probably due to the higher amount of the paramagnetic ions, Cu(II). The changed slope indicates that the higher concentration decreases the sensitivity of the system. Further investigations have to be performed to find the optimal concentrations for the system.

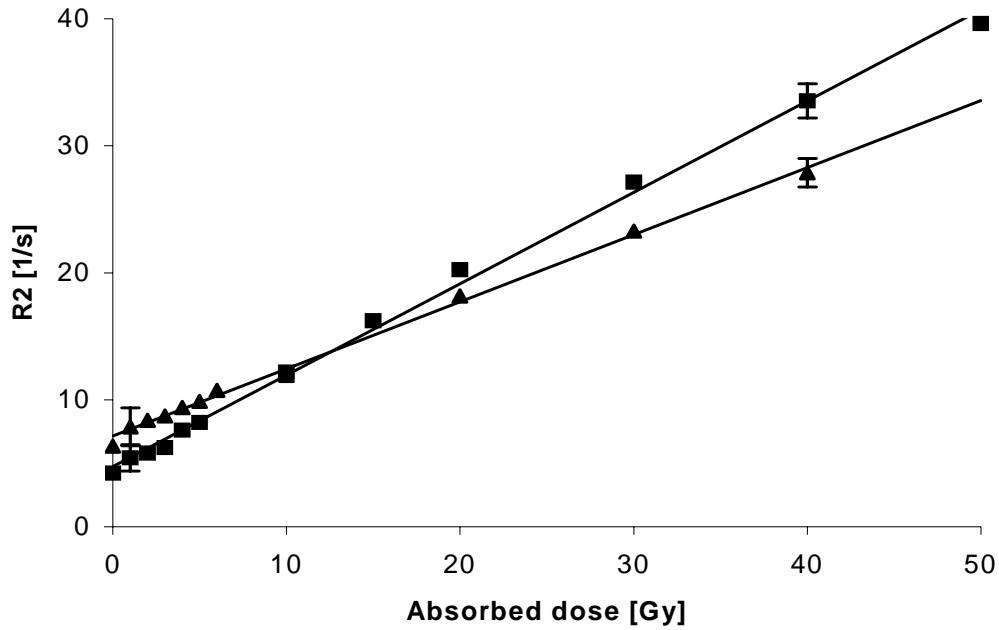


Figure 12. R2 dose response for different amounts of Ascorbic acid and copper sulphate. AA 4×10^{-3} M and CuSO_4 $6,6 \times 10^{-4}$ M (▲), AA 2×10^{-3} M and CuSO_4 $3,3 \times 10^{-4}$ M (■). The evaluation was performed using the Praxis analyser. (MAA (M 0782) 8 % for both).

Table 5. Concentrations of ascorbic acid and copper sulphate, slope, intercept and correlation coefficient for the graphs in figure 12.

Conc. AA [M]	Conc. Cu(II) [M]	Slope [$\text{s}^{-1}\text{Gy}^{-1}$]	Intercept [s^{-1}]	R^2
4×10^{-3}	$6,6 \times 10^{-4}$	0,528	7,150	0,997
2×10^{-3}	$3,3 \times 10^{-4}$	0,720	4,738	0,997

The optimal gel composition (highest slope, the lowest intercept and linearity from 0 Gy) prepared during these investigations was the gel with 8 % of methacrylic acid (M 0782), 2×10^{-3} M ascorbic acid and $3,3 \times 10^{-4}$ M copper sulphate.

Uncertainty estimation

The uncertainty estimation was performed according to the recommendations by ISO 1995 [30]. The uncertainty from evaluating the same sample several times was referred to as type A1. Type A2 was the uncertainty when several samples were irradiated to the same absorbed dose. This was assumed to be only due to the chemical condition of the different samples. Accordingly, this uncertainty is considered to be the same both for the Praxis analyser and the MRI scanner. Type B uncertainties that have to be estimated [30] were the uncertainties rising from temperature differences between batches and the accelerator performance. For the MRI scanner the non-uniformity was included in this uncertainty as well. When estimating the uncertainty due to temperature differences it was assumed that OPoG responds in the same way as PoG. The measurements performed by Maryanski *et al* were used [31].

Table 6. The values for the type A and B uncertainty estimations in R2 [s^{-1}]. For the Praxis analyser $R2(1\text{ Gy})=6.9\text{ s}^{-1}$ and $R2(40\text{ Gy})=34.2\text{ s}^{-1}$, for the MRI scanner $R2(1\text{ Gy})=4.1\text{ s}^{-1}$ and $R2(40\text{ Gy})=20.4\text{ s}^{-1}$.

Evaluation method	Type A1 [SD]		Type A2 [SD]		Type B [SD]	
	1 Gy	40 Gy	1 Gy	40 Gy	1 Gy	40 Gy
Praxis analyser	0.31	0.33	0.56	0.56	0.14 (acc.)	0.35 (acc.)
					0.2 (temp.)	0.4 (temp.)
MRI scanner	0.10	0.67	0.51	0.51	0.08 (acc.)	0.11 (acc.)
					0.2 (temp.)	0.4 (temp.)
					0.24 (non-uni.)	0.31 (non-uni.)

The type B uncertainties were assumed to have a distribution that is approximately gaussian. The uncertainties (type A and B) were combined according to ISO 1995 [30]. A 95 % confidence limit was obtained by multiplying the combined standard deviation by the coverage factor 2.

Table 7. The expanded standard uncertainty for the dose response of 1 and 40 Gy in figure 10. The percentage standard uncertainty was used for the error bars in figure 8, 9 and 12.

Evaluation method	Expanded standard uncertainty. [SD]	
	1 Gy	40 Gy
Praxis analyser	1.3 s^{-1} (19 %)	1.4 s^{-1} (4 %)
MRI scanner	1.1 s^{-1} (26 %)	2.0 s^{-1} (10 %)

The basis for the R1 uncertainty estimation was the same as for R2, pursuing the recommendations of ISO 1995 [30]. The uncertainties referred to as A2 and B were translated roughly by percent from R2 to R1. Type A1 was evaluated by measuring the same sample several times.

Table 8. The values for the type A and B uncertainty estimations in R1 [s^{-1}]. For the Praxis analyser $R1(1\text{ Gy})=1.3\text{ s}^{-1}$ and $R1(40\text{ Gy})=2.8\text{ s}^{-1}$.

Evaluation method	Type A1 [SD]		Type A2 [SD]		Type B limits	
	1 Gy	40 Gy	1 Gy	40 Gy	1 Gy	40 Gy
Praxis analyser	0.05	0.04	0.1	0.1	0.01 (acc.)	0.03 (acc.)
					0.02 (temp.)	0.03 (temp.)

Table 9. The expanded standard uncertainty for the dose response of 1 and 40 Gy sample in figure 8, the error bars are too small to be visible in the figure.

Evaluation method	Expanded standard uncertainty. [SD]	
	1 Gy	40 Gy
Praxis analyser	0.11 s^{-1} (8.5 %)	0.11 s^{-1} (4.0 %)

By using these estimated uncertainties and the slopes of the dose response in figure 8 a dose resolution of the measurements was approximated. The dose resolution was defined as the standard deviation of the measured values (R1 and R2) divided by the slope of the dose response (R1- and R2 vs. absorbed dose). For the evaluations performed the dose resolution

was 5.6 Gy for R1 and 2.6 Gy for R2 (Table 10). Due to the superior dose resolution R2 is the most common used evaluation parameter with NMR/MRI for gel dosimetry.

Table 10. Standard deviation, slope and dose resolution for the R1 and R2 absorbed dose response.

Parameter	SD [s^{-1}]	Slope [$s^{-1}Gy^{-1}$]	Dose resolution
R1	0.22	0.04	5.6
R2	1.4	0.53	2.6

5.8 MRI non-uniformity

Non-uniformity was discovered not to be a pronounced problem for the phantom and the MRI measurements used. The R2 values did not differ more than 2 % in the area of interest (fig. 13). It was only close to the edges greater differences were found. These results are in agreement with previously reported results [23].

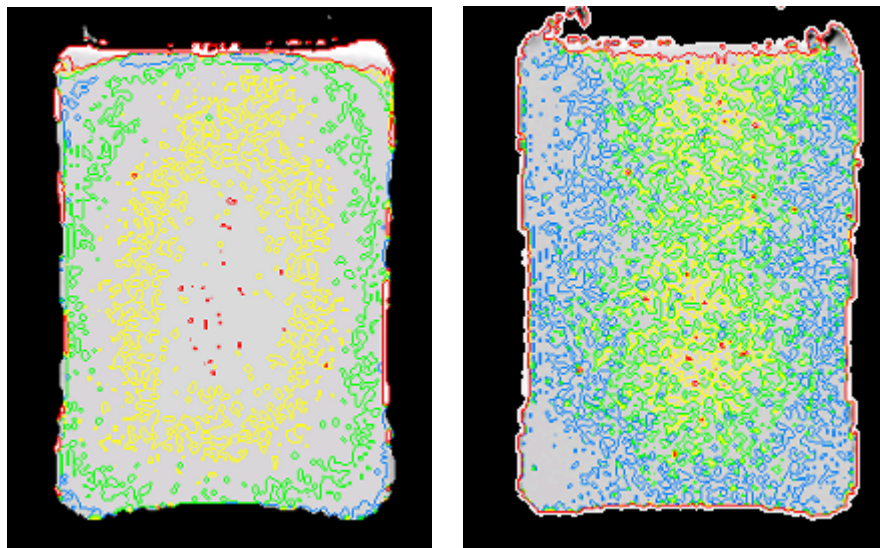


Figure 13. Investigation of non-uniformities in the image of R2. Gel phantoms produced to simulate 0 Gy (left) and 30 Gy (right) Gy. (blue - 98 %, green – 99 %, yellow – 100 %, red – 101 %)

5.9 IMRT verification

An area of 4 pixels containing values of 100 % in the calculated TPS dose distribution was chosen for the normalisation. The same area in the image of the relative dose from the measurement was identified. The values of the area in the measurements were found to be constant. This justified the 4-pixel-area normalisation procedure (fig. 14).

Normalisation region

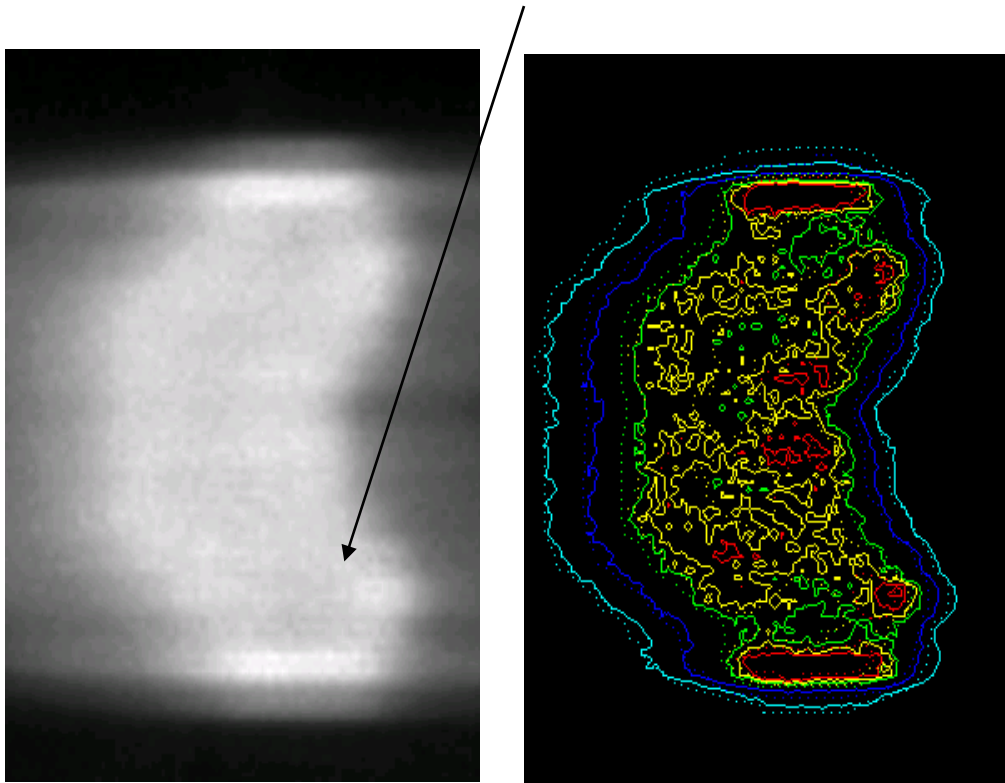


Figure 14. The grey scaled image of the measured relative dose map (R2 map) (left) of the IMRT irradiation. Isodoses for the measured relative absorbed dose map (solid) and the calculated dose map from the treatment planning system (dotted) (right). (light blue-60 %, blue- 75 %, green-95 %, yellow- 100 %, red-105 %).

The treatment plan and the measured relative absorbed dose were found to be in good accordance (fig. 14). The 60 %, 75 % and 95 % isodose lines were mostly within 2 mm of agreement. For isolated regions the difference was approximately maximum 3 mm. The calculation performed by the TPS, accelerator output and the measurement are uncertainty factors.

Our results indicate that there are a great potential for gel dosimetry for this type of measurements. However another type of image processing may make it easier to quantify the differences between the treatment plan and the measured absorbed dose. The development of an evaluation method for such quantification was beyond the scope of this thesis.

It is not reasonable to obtain an absolute absorbed dose calibration for gel dosimetry. There are too many factors of uncertainty involved. The absorbed dose calibration is carried out in small screw-top glass vials, whereas the phantom is rather big. Other solutions have been suggested [32]. When evaluating the vials in the MRI scanner, they are placed in the centre of the head coil surrounded by air instead of gel or some other material with similar NMR characteristics. Even if they were surrounded by gel, the glass vial would still be there. As absolute absorbed dose calibration is not an option, thus the calibration has to be relatively. When using relative absorbed dose calibration linear relationship is required. The normalisation procedure will thus be very important for the interpretation of the result and it also determine which of the isodose lines to agree and which to disagree.

When further IMRT verifications were undertaken a problem was discovered. “Cloudiness” and “structures” were present in the images of the gel phantom (fig. 15). Neither for PoG or

OPoG has these problems been reported before. These problems were also seen visually in the gel.

It is not likely that this problem is due to gelatine or Cu(II) alone, as those components are used in the non-uniformity study and the “cloudiness” and “structures” did not arise there. The two acids that is used in the dosimetry gel, ascorbic acid and methacrylic acid, results in pH-value 3 approximately. So that should not be a problem either i.e. the gel could not be degraded by the acid (Fricke gels have a pH-value of approximately 1). Further investigations regarding the manufacturing process are needed. The methacrylic acid may not be completely solved; the same can be true for the ascorbic acid.

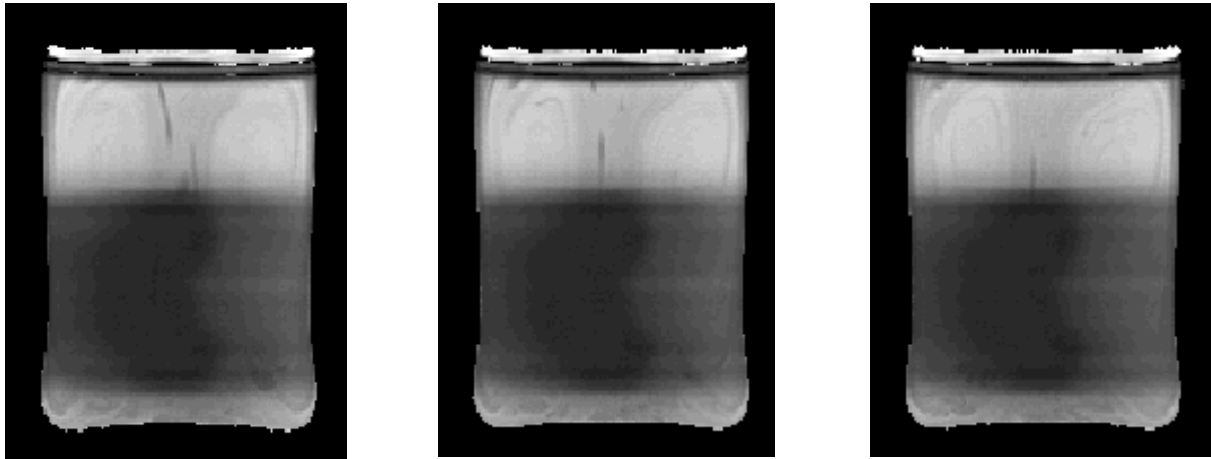


Figure 15. *T2 maps of the gel phantom, the image in the middle shows the isocentric slice, the two other images are showing the slice just behind and the slice just in front. The phantom has been irradiated with the planned IMRT. The grey-scale is set to show the “cloudiness” and “structures” out side the target area.*

Because of the “cloudiness” and “structures” the agreement between the treatment plan and the measured relative absorbed dose was not so good (fig. 16). This was due to that regions with these inhomogeneities suffer from incorrect measured absorbed dose, both over- and under estimations occur.

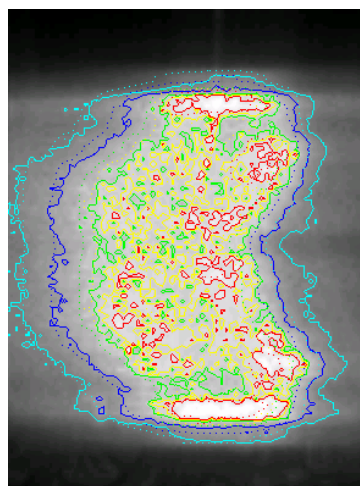


Figure 16. *The grey scaled image of the measured relative absorbed dose. Isodoses for the measured relative absorbed dose map (solid) and the calculated dose map from the treatment planning system (dotted). (light blue-60 %, blue- 75 %, green-95 %, yellow- 100 %, red-105 %)*

Conclusions

The total time for the presented mixing procedure is approximately 2 h. The short mixing time is mostly due to that there is no need to prevent oxygen from getting in contact with the gel. This is a great improvement compared to PoG. For the investigations made upon the dose response it was found that the selection of methacrylic acid was crucial for the linearity from 0 Gy absorbed dose. The amount of ascorbic acid and copper sulphate were also found to influence the dose response. Lower amounts increased the sensitivity, though this may only be valid for the amounts examined. Further investigations are needed to find the optimal amounts of ascorbic acid and copper sulphate.

With the exception of the extended linear range (40 Gy) the OPoG characteristics were found to be similar as for PoG. However OPoG has the advantages of not being hypoxic and the ingredients are less toxic than for PoG [7].

MRI signal non-uniformities were found to not be a pronounced problem. In the area of interest the R2 value did not differ more than 2-3 % for the homogenous phantom.

For the IMRT verification the treatment plan and the measured relative absorbed dose distributions were found to be in good agreement. The isodose lines were mostly within 2 mm of agreement. For isolated regions the difference was approximately maximum 3 mm. The results of this study indicate that there are a great potential for gel dosimetry for IMRT measurements. However there is a need for further optimisation of the gel composition and to lower the uncertainty in the measured absorbed dose. There is a need of further investigations to solve the “cloudiness” and “structure” problems.

6 Acknowledgements

This thesis is the result of a graduate project for a degree of Master of Science in radiation physics. The project has been carried out at the Department of Radiation Physics, Lund University, Malmö University Hospital, during the autumn 2001.

I want to thank the following people:

My supervisor Sven ÅJ Bäck for really caring and being nice and positive.

Helen Gustavsson for being my "additional supervisor" and my friend. I could not have had a better guide on my first trip abroad.

Lars E Olsson for helping me with the MRI measurements and the remarks on my thesis.

Pia Haraldsson and Terje Andersen (and the rest of the staff involved) for all the help in Copenhagen (and by e-mail).

Jonas Svensson for helping me with all kinds of computer problems.

My "roomies" Helen, Jonas and David for keeping me company. There is no one else I rather would share the office with.

A special thank to the Department of Radiation Physics in Malmö, for giving me the opportunity (and money) to participate in DOSGEL 2001, Brisbane, Australia.

I also want to thank Helen (again), Erica Bloom and Simon Steiner for taking good care of Eddie when I was working on my thesis.

7 References

1. The Swedish council on Technology Assessment in Health Care *Strålbehandling vid cancer*. Stockholm: SB offset AB; 1996:1.
2. Webb S. *The physics of conformal radiotherapy. advances in technology*. London: Institute of Physics Publishing, The Institut of Physics; 1997.
3. ICRU. Report No. 50. *Prescribing, recording, and reporting photon beam therapy*. Betesda, MD: ICRU Publications; 1993.
4. Bäck SÅJ. *Implementation of MRI gel dosimetry in radiation therapy*. Malmö: Lund University, PhD Thesis; 1998.
5. Webb S. *Intensity-Modulated Radiation Therapy*. London: Institute of Physics Publishing, The Institute of Physics; 2001.
6. Keall P. *et al* A theoretical study of the radiological properties and water equivalence of Fricke and polymer gels used for radiation dosimetry. *Australas Phys Eng Sci Med* 1999; 22(3):85-91.
7. Fong PM. *et al* Polymer gels for magnetic resonance imaging of radiation dose distributions at normal room atmosphere. *Phys Med Biol* 2001; 46(12):3105-3113.
8. Gore JC, Kang YS, Schulz RJ. Measurement of radiation dose distributions by nuclear magnetic resonance (NMR) imaging. *Phys Med Biol* 1984; 29(10):1189-1197.
9. Olsson LE, Westrin BA, Fransson A, Nordell B. Diffusion of ferric ions in agarose dosimeter gels. *Phys Med Biol* 1992; 37:2243-2346.
10. Maryanski MJ. *et al* NMR relaxation enhancement in gels polymerized and cross-linked by ionizing radiation: a new approach to 3D dosimetry by MRI. *Magn Reson Imaging* 1993; 11(2):253-258.
11. Maryanski MJ, Schulz RJ, Ibbott GS, Gatenby JC, Xie J, Horton D, Gore JC. Magnetic resonance imaging of radiation dose distributions using a polymer-gel dosimeter. *Phys Med Biol* 1994; 39:1437-1455.
12. Lepage M, Whittaker AK, Rintoul L, Baldock C. ¹³C-NMR, ¹H-NMR and FT-Raman Study of Radiation Induced Modifications in Radiation Dosimetry Polymer Gels. *Journal of Applied Polymer Science* 2001; 79:1572-1581.
13. Gustavsson H, Bäck SÅJ, Olsson LE. A polymer gel prepared under normal levels of oxygenation: Basic studies. *Preliminary Proceedings of DOSGEL 2001 2nd International Conference on Radiotherapy Gel Dosimetry* 2001; s 98-100.
14. Haraldsson P. *et al* Dose response characteristics and basic dose distribution data for a polymerization-based dosimeter gel evaluated using MR. *Br J Radiol* 2000; 73(865):58-65.
15. Baldock C. *et al* Fourier transform Raman spectroscopy of polyacrylamide gels (PAGs) for radiation dosimetry. *Phys Med Biol* 1998; 43(12):3617-3627.
16. Gore JC. *et al* Radiation dose distributions in three dimensions from tomographic optical density scanning of polymer gels: I. Development of an optical scanner. *Phys Med Biol* 1996; 41(12):2695-2704.
17. Hilts M. *et al* Polymer gel dosimetry using x-ray computed tomography: a feasibility study. *Phys Med Biol* 2000; 45(9):2559-2571.
18. Mather ML, Whittaker AK, Baldock C. Ultrasound-a new method for evaluation of polymer gel dosimeters. *Preliminary Proceedings of DOSGEL 2001 2nd International Conference on Radiotherapy Gel Dosimetry* 2001; s 181-183.

19. Lepage M. Modelling of post-irradiation events in polymer gel dosimeters. *Phys Med Biol* 2001; 46(11):2827-2839.
20. Gangi Reddy G, Nagabhushanam T, Santappa M, Venkata Rao K. Oxygen-Ascorbic Acid-Copper(II) Initiating System. A Kinetic Studie of the Polymerisation of Methyl Acrylate in Aqueous Medium. *Makromol Chem* 1982; 183:905-913.
21. Schreiner LJ. Fricke gel dosimetry. *Preliminary Proceedings of DOSGEL 2001 2nd International Conference on Radiotherapy Gel Dosimetry* 2001; s 15-22.
22. Magnusson P. *MRI evaluation and Image processing in Gel dosimetry*. Malmö: Lund University, PhD Thesis; 2001.
23. De Deene Y. Fundamentals of MRI measurements for gel dosimetry. *Preliminary Proceedings of DOSGEL 2001 2nd International Conference on Radiotherapy Gel Dosimetry* 2001; s 49-65.
24. De Deene Y. Artefacts in multi-echo T2 imaging for high-precision gel dosimetry: III. Effects of temperature drift during scanning. *Phys Med Biol* 2001; 46(10):2697-2711.
25. Lepage M. *et al* Simple methods for the correction of T2 maps of phantoms. *Magn Reson Med* 2001; 46(6):1123-1129.
26. Varian Medical Systems. *CadPlan Using Helios and Electronic Compensator. user manual*
27. ICRU. Report no 42. *Use of Computers in External Beam Radiotherapy Procedures with High Energy Photons and Electrons*. Bethesda MD: ICRU Publications; 1987.
28. Lepage M, Jayasakera PM, Bäck SÅJ, Baldock C. Dose resolution optimization of polymer gel dosimeters using different monomers. *Phys Med Biol* 2001; 46:2665-2680.
29. Lepage M, Bäck SÅJ, Jayasekera PM, Baldock C. Optimizing the dose resolution in polymer gel dosimetry. *Preliminary Proceedings of DOSGEL 2001 2nd International Conference on Radiotherapy Gel Dosimetry* 2001; s 178-180.
30. ISO Guide to the Expression of Uncertainty in Measurements 1995
31. Maryanski MJ. *et al* Effects of crosslinking and temperature on the dose response of a BANG polymer gel dosimeter. *Phys Med Biol* 1997; 42(2):303-311.
32. Oldham M. *et al* Improving calibration accuracy in gel dosimetry. *Phys Med Biol* 1998; 43(10):2709-2720.
33. De Deene Y. *et al* An investigation of the chemical stability of a monomer/polymer gel dosimeter. *Phys Med Biol* 2000; 45(4):859-878.